AD-A073 078 ROME AIR DEVELOPMENT CENTER GRIFFISS AFB NY F/G 17/9

AN EVALUATION OF SOME FACTORS AFFECTING THE CHOICE OF OPERATING--ETC(U)

MAR 79 J L POIRIER

UNCLASSIFIED RADC-TR-79-83 NL

1 OF 1

AD A073078

END

DATE FILMED

9-79

DDC

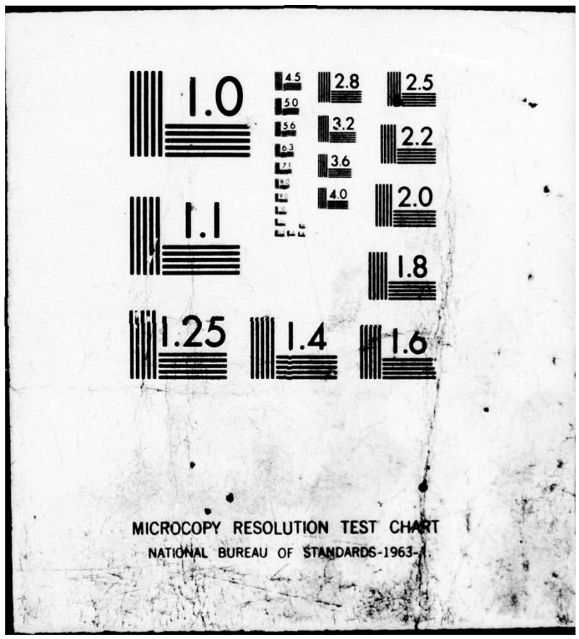
1.0
1.1
1.25
1.4
1.6
1.8
2.0
2.2
2.5
2.8
3.2
3.6
4.0
4.5
5.0
5.6
6.3
7.1
MICROCOPY RESOLUTION TEST CHART
NATIONAL BUREAU OF STANDARDS-1963-A

LEVEL II

(12)
B.S.

RADC-TR-79-83
In-House Report
March 1979

ROME AIR DEVELOPMENT CENTER

AN EVALUATION OF SOME FACTORS AFFECTING THE CHOICE OF OPERATING FREQUENCY OF A GUIDED WAVE RADAR FOR INTRUDER DETECTION

J. Leon Poirier

ROME AIR DEVELOPMENT CENTER
Air Force Systems Command
Griffiss Air Force Base, New York 13441

This report has been reviewed by the RADC Information Office (OI) and is releasable to the National Technical Information Service (NTIS). At NTIS it will be releasable to the general public, including foreign nations.

RADC-TR-79-83 has been reviewed and is approved for publication.

APPROVED: Philipp Blacksmith

PHILIPP BLACKSMITH
Chief, EM Systems Concepts Branch

APPROVED: William Baschnagel

WILLIAM R. BASCHNAGEL, Lt Colonel, USAF
Assistant Chief
Electromagnetic Sciences Division

Accession For	
NTIS GRA&I	X
DDC TAB	
Unannounced	
Justification	
By	
Distribution/	
Availability Codes	
Dist	Avail and/or special
A	

FOR THE COMMANDER: John P Huss

JOHN P. HUSS
Acting Chief, Plans Office

If your address has changed or if you wish to be removed from the RADC mailing list, or if the addressee is no longer employed by your organization, please notify RADC (EEC) Hanscom AFB MA 01731. This will assist us in maintaining a current mailing list.

Do not return this copy. Retain or destroy.

MISSION
of
Rome Air Development Center

RADC plans and executes research, development, test and selected acquisition programs in support of Command, Control Communications and Intelligence (C^3I) activities. Technical and engineering support within areas of technical competence is provided to ESD Program Offices (POs) and other ESD elements. The principal technical mission areas are communications, electromagnetic guidance and control, surveillance of ground and aerospace objects, intelligence data collection and handling, information system technology, ionospheric propagation, solid state sciences, microwave physics and electronic reliability, maintainability and compatibility.

Printed by
United States Air Force
Hanscom AFB, Mass. 01731

Unclassified

SECURITY CLASSIFICATION OF THIS PAGE (When Data Entered)

REPORT DOCUMENTATION PAGE | READ INSTRUCTIONS BEFORE COMPLETING FORM

14

1. REPORT NUMBER: RADC-TR-79-83
2. GOVT ACCESSION NO.
3. RECIPIENT'S CATALOG NUMBER

6

4. TITLE (and Subtitle): AN EVALUATION OF SOME FACTORS AFFECTING THE CHOICE OF OPERATING FREQUENCY OF A GUIDED WAVE RADAR FOR INTRUDER DETECTION
5. TYPE OF REPORT & PERIOD COVERED: In-House Report
6. PERFORMING ORG. REPORT NUMBER

10

7. AUTHOR(s): J. Leon Poirier
8. CONTRACT OR GRANT NUMBER(s)

17 15

9. PERFORMING ORGANIZATION NAME AND ADDRESS:
Deputy for Electronic Technology (RADC/EEC)
Hanscom AFB
Massachusetts 01731

16

10. PROGRAM ELEMENT, PROJECT, TASK AREA & WORK UNIT NUMBERS: 46001501

11. CONTROLLING OFFICE NAME AND ADDRESS:
Deputy for Electronic Technology (RADC/EEC)
Hanscom AFB
Massachusetts 01731

11

12. REPORT DATE: Mar[redacted]79
13. NUMBER OF PAGES: 31

14. MONITORING AGENCY NAME & ADDRESS (if different from Controlling Office)

12 32p.

15. SECURITY CLASS. (of this report): Unclassified

15a. DECLASSIFICATION/DOWNGRADING SCHEDULE

16. DISTRIBUTION STATEMENT (of this Report)

Approved for public release; distribution unlimited.

62702F

17. DISTRIBUTION STATEMENT (of the abstract entered in Block 20, if different from Report)

18. SUPPLEMENTARY NOTES

19. KEY WORDS (Continue on reverse side if necessary and identify by block number)

Leaky coaxial cable
Intrusion sensors
Guided wave radar

20. ABSTRACT (Continue on reverse side if necessary and identify by block number)

The detection sensitivity of a guided wave radar designed to detect intruders crossing a perimeter up to two miles long is analyzed. Expressions are developed for the signal-to-noise ratio as a function of operating frequency and system properties. It is shown that performance is degraded as the operating frequency increases. The principal reason for this is the rapid rise in the attenuation of parallel leaky coaxial cables used as guided wave structures. The results indicate that satisfactory performance of such systems could be expected at frequencies up to 100 or 200 MHz. However, improved → next page

DD FORM 1 JAN 73 1473 EDITION OF 1 NOV 65 IS OBSOLETE

Unclassified

SECURITY CLASSIFICATION OF THIS PAGE (When Data Entered)

309050

Gm

20. (Cont)

sensitivity is obtained at lower frequencies.

Contents

Illustrations

Illustrations

Tables

An Evaluation of Some Factors Affecting the Choice of Operating Frequency of a Guided Wave Radar for Intruder Detection

1. INTRODUCTION

The purpose of this study is to estimate the degradation in performance of the Guidar ported coaxial cable* sensor system[1] at frequencies outside the initial design range of 50 to 100 MHz. The principal cause for reduced performance as the operating frequency is increased is the rapid rise in the attenuation of the ported coaxial cable sensor. In contrast, below about 50 MHz, the scattering cross section of an intruder begins to decrease. Thus there is a region below and above which the ported coaxial cable sensor system does not operate to the best advantage.

A simplified diagram of the ported coaxial cable sensor to be discussed is shown in Figure 1. It consists of a transmitter module connected to a leaky (ported) cable about a mile long. A similar receiving cable parallel to and separated a few feet from the transmitting cable is connected to a receiving module. Each of the sensor cables is made up of three identical sections about 2000 ft long. Line amplifiers

(Received for publication 29 March 1979)

*The term "Guidar" has been coined by Computing Devices Company of Canada for its guided wave radar intrusion detection system. The appellation "ported coaxial cable" has been applied by the Electronic Systems Division to the class of leaky coaxial cable used in the Guidar system.

1. Harman, R.K. (1976) GUIDAR: An intrusion detection system for perimeter protection, Proc. 1976 Carnahan Conference on Crime Countermeasures, University of Kentucky, Lexington, Ky.

are used to amplify the signal levels between each section in order to offset the decrease in signal strength caused by attenuation.

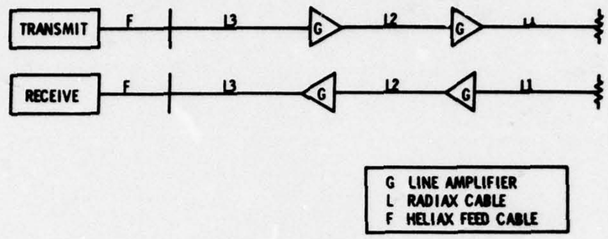

Figure 1. Simplified Block Diagram of Guidar (Guided Wave Radar)

A sketch of a section of ported coaxial cable is shown in Figure 2. Many such cables are available and details of the type shown in this sketch are peculiar to the cable used in the Guidar system. A number of holes have been cut in the solid outer conductor of the cable to allow a small fraction of the radio frequency energy traveling on the inside to "leak" out and propagate along the outside of the cable. It is the interaction of an intruder with this external field that allows detection and location of an intrusion.

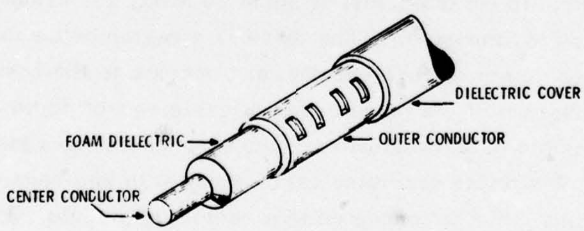

Figure 2. Construction Details of Ported Coaxial Cable

Operation of the system is similar to that of a pulsed radar system, except that the signals propagate along the cables rather than radiate through space. In the absence of an intruder, the energy coupled from one region of the transmitting cable to the adjacent receiving cable depends on cable properties, as well as the ground conditions there. This steady signal corresponds to the clutter return of a conventional radar. The extent of the region (range resolution cell) depends on the pulse width. The level of the signal returned from each point along the cable is stored in the Guidar processor and updated in order to account for slow changes in ambient conditions.

When an intruder approaches within a few feet of the cable sensor, the signal return corresponding to that range bin is modified. This new value is subtracted from the value previously stored in the processor. The effect of the subtraction is cancellation of the clutter background and production of an output proportional to the modification signal level produced by the intruder. In this way, an intrusion is detected and located. Actual system operation is, of course, more sophisticated, although not the fundamental concept. It is the sensitivity to detect intruders as the operating frequency is changed that will be examined in this analysis.

A parameter which can be used to characterize system performance is the signal-to-noise (S/N) ratio at the input to the receiver This quantity is fundamental in estimating the detection sensitivity of any radar. For this system, the signal power S at the receiver input is

$$S = P_o - 2A_F - 2A - K - C \tag{1}$$

where P_o is the transmitter power, A_F is the attenuation of one of the feeder cables, 2A the ported coaxial signal attenuation, K the cable-to-cable coupling loss, and C the intruder cross section loss. With exception of P_o, each of these parameters depends on frequency. In addition, S depends on the location of the perturbing intrusion since A and K (as will be explained later) depend on the distance from the cable input to the point of intrusion.

The noise power N originates from a number of sources, including the line amplifiers in the receiving sensor and the thermal noise generated in the loads that terminate the cables. The net noise power which reaches the receiver input depends on cable losses, making the noise power N also a function of frequency.

Once the S/N ratio has been established, it is possible to compute the detection properties of the system. These will be compared to a standard system that operates at 60 MHz.

In the next sections, each of the system properties discussed in the foregoing paragraphs will be analyzed, in order to determine the impact on system performance.

2. ATTENUATION FACTOR

The attenuation of a length of coaxial cable is usually computed from its attenuation factor without regard to location of the cable. However, since ported coaxial cables are designed to leak off some energy, they are somewhat affected by their environment. Thus their electrical properties change with both frequency and location. Representative values for Radiax[2] cable types RX4-1 and RX4-3 are shown in Figures 3 and 4, respectively. The solid curves apply when the cables are supported well away from the ground (free space). The RX4-1 cable has smaller holes in its outer sheath conductor as compared to the RX4-3; as a consequence, the attenuation factor of the former is correspondingly smaller. The dashed curves (Figure 3) show the effect of placing the cables near a lossy medium. The attenuation factor for RX4-1 is seen to be less affected by the location of the cable, as compared to RX4-3, because of its smaller hole size. Properties of the lossy medium such as soil type and moisture content affect the value of the attenuation factor; for example, the attenuation measured in a length of cable buried six inches below the surface decreased to near free space values when the ground was solidly frozen. In addition, small variances in attenuation factor occur as the result of manufacturing tolerances. Nevertheless, the data shown in Figures 3 and 4 indicate a general agreement among workers in the field on the value of attenuation to be expected from Radiax cable. This cannot be said for the coupling loss described in the next section.

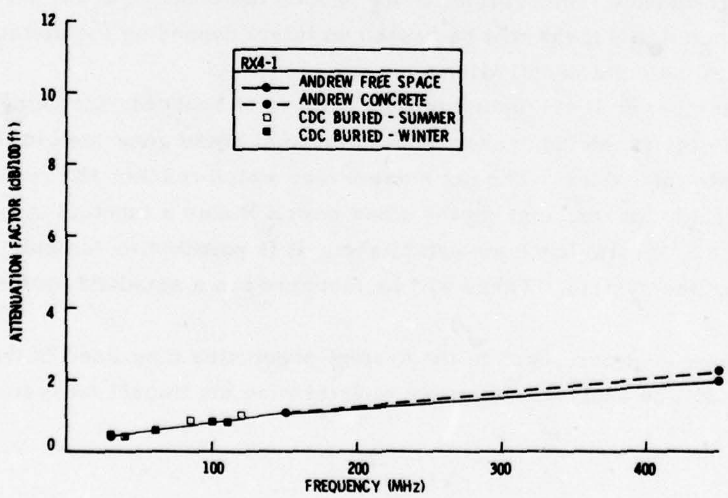

Figure 3. Attenuation Factor for RX4-1 Radiax Cable

2. Bulletin 1058A, Radiax Slotted Coaxial Cable, Andrew Corporation, Orland Park, Ill.

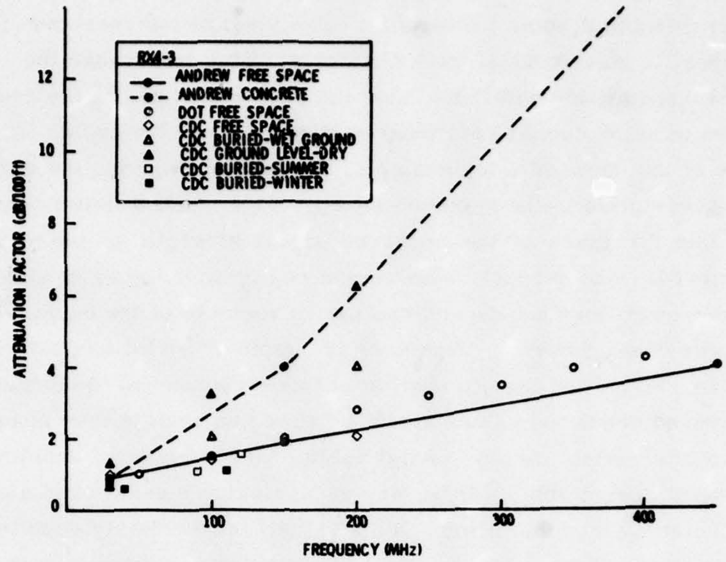

Figure 4. Attenuation Factor for RX4-3 Radiax Cable

Low-loss coaxial cables, for example, Heliax[3] are used for the feeder cables. The attenuation factor for Heliax 1/2-in. diam cable is the same as that for RX4-1.

3. COUPLING LOSS

The coupling loss normally associated with these cables is defined as

$$K' = 10 \log \frac{P_o}{P_r} \qquad (2)$$

where P_o is the power at the input to the cable and P_r the power received by a half-wave dipole antenna located some distance from the cable. In practice, the value observed varies considerably as the probing antenna is moved either parallel to or transverse to the transmitting cable. Typical of the results observed are the curves shown in Figure 5. There is significant structure to the patterns and deep nulls are evident. The received power tends to decrease as $1/r$ or $1/r^2$ depending on the frequency and length of the cable as the probing antenna is moved away from the cable. The fields surrounding leaky coaxial cables cannot be accurately predicted

3. Catalog 28, Antennas/Transmission Lines, Andrew Corporation, Orland Park, Ill.

although they do exhibit some periodicity. The level of the received signal depends chiefly on specific placement of the leaky cable. This is because the cable acts as a distributed transmitting antenna. Thus the received signal is the result of the superposition of many components from various parts of the cable. A change in the phase of one of the dominant, for example, produced by moving the cable can cause a large variation in the received signal. This phase related dependence effects the fine structure of the observed signal strength as the probing antenna is moved. The average value over a region is not greatly affected since the total radiated power does not depend on exact placement of the cable. The average received power does, however, depend on the depth of burial and nature of the soil which, in turn, determine the attenuation of the fields around the cables. Variations of ± 10 dB around predicted values are to be expected even in free space.

To make this variable leaky coaxial cable characteristic of coupling loss more useful in system design applications, an average value measured in a specified manner is quoted by manufacturers. This value, called simply coupling loss, is obtained by Andrew Corporation by averaging the loss measured as the dipole is moved over a range of 10 to 30 ft from the cable. The resulting value is taken to be the value ± 10 dB which would be observed 20 ft from the cable. This quantity, used in the system analysis, will be discussed in connection with Figures 6 and 7.

The coupling loss for RX4-1 is shown in Figure 6. The data for this curve was obtained from the Radiax cable data sheets. Figure 7 shows the results of measurements of RX4-3, as reported from several sources. Some discussion is required at this point: First, inspection of Figure 6 shows that there is no change in coupling (average) as the RX4-1 cable is moved from free space to the ground. This is consistent with the findings of Cree and Giles[4]—that a cable in which the attenuation factor is insensitive to position exhibits very little change in coupling loss as its position is varied. However, in contrast, the lower two curves in Figure 7 clearly show a change in coupling as the RX4-3 cable is moved; in fact, the enormous spread in reported data indicates the sensitivity of the measurement to specific conditions. First, it should be pointed out that the values for coupling loss in the Andrew Corporation data are obtained by them by averaging coupling loss measured near the center of a 100-ft cable for distances 10 to 30 ft away from the cable. The coupling loss for the Department of Transportation (DOT) data are obtained by averaging their measured values in a similar way.

4. Cree, D.J., and Giles, L.J. (1975) Practical performance of radiating cables, Radio Elec. Eng. **45**(No. 5):221-225.

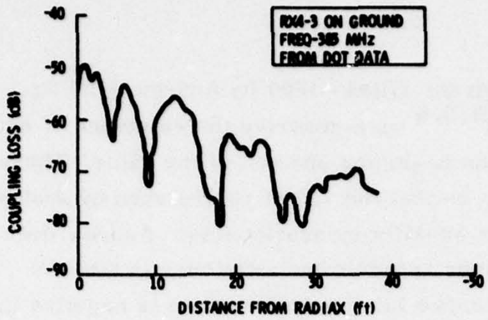

Figure 5. Variation of Coupled Signal Power with Distance from Leaky Coaxial Cable

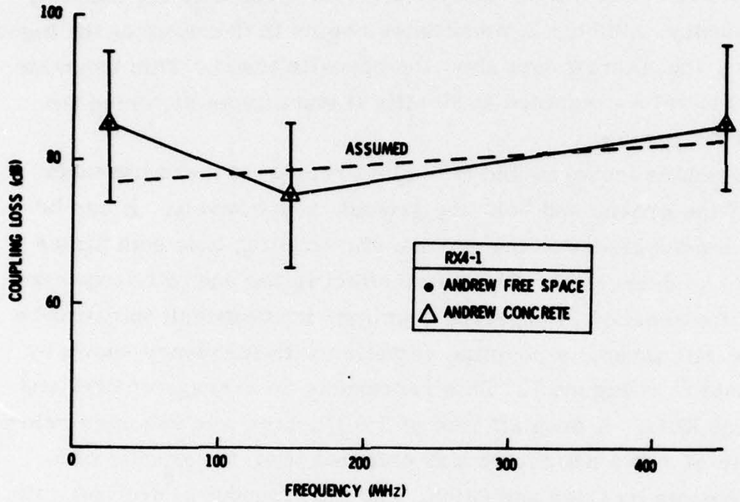

Figure 6. Variation of Coupling Loss with Frequency for RX4-1

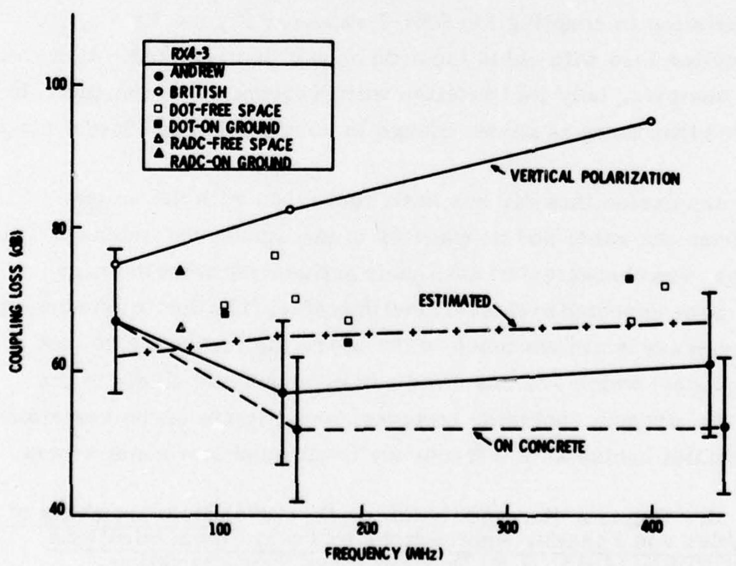

Figure 7. Variation of Coupling Loss with Frequency for RX4-3

The following cable lengths have been given: Giles—1600 ft; Andrew—100 ft; and DOT—100 to 200 feet. Several workers[3,5,6] have reported the existence of end effects that can modify the field pattern at the beginning and end of the cable. These effects can persist for several wavelengths, so that the 100-ft cables used by Andrew and the DOT may have been too short for the 30-MHz measurements. Andrew does place a ± 10 dB range on their values. Another apparent inconsistency is that the slope of the coupling loss versus frequency curve for the Andrew data is negative in the range 30 to 150 MHz. Cree and Giles have made measurements on a large number of leaky coaxial cables of many types. They found that invariably the coupling loss increased with frequency, although it sometimes begins to decrease at the higher frequencies. In contrast, the Andrew data show the opposite trend. This behavior could be connected with the values obtained at 30 MHz if end effects distorted the fields near the center of the cables.

The open and solid symbols (squares and triangles) represent measurements made with the cable "off" the ground and "on" the ground, respectively. It can be seen that as the cable is moved closer to the ground, the coupling loss sometimes increases and at other times decreases. The latter effect is the one to be expected.

In view of the large discrepancy in expected coupling, it is difficult to estimate actual performance. We will assume a coupling variation with frequency shown by the curve labeled "estimated" in Figure 7. This represents an average of DOT and Andrew values down to 150 MHz. A drop off rate of 2 dB/octave was assumed below 150 MHz. A drop off rate of 3 to 5 dB/octave was obtained from the results of a large number of measurements by Cree and Giles, who also found this drop off rate to be the same for many different types of cables. Similar arguments were used to select the "assumed" variation in coupling for RX4-1 shown in Figure 6.

The variation in coupling loss with cable location cannot be predicted. However, for the purposes of this analysis, only its variation with frequency is important. It will therefore be assumed that there is no net change in coupling loss when the leaky cable is buried.

In this section, the discussion thus far has been concerned with the amount of energy lost as it leaks from the cable and propagates to the dipole test antenna. This quantity, the coupling loss, was characteristic of a cable and describes the average strength of the field that can be expected to exist around the cable. The dipole antenna which is used in these measurements is always tuned to the operating frequency so that the variations (with frequency) which are observed can be attributed solely to the leaky coaxial cable. In the present analysis, however, an estimate of the variation coupling between two parallel cables as the frequency is changed is a requirement.

---

5. Yoh, P., Esposito, R., Gagnon, R., and Kodis, R.D. (1974) Measurements of Leaky Coaxial Cables and Possible Applications to Train Communications, Report No. FRA-ORD&D-74-43, U.S. Department of Transportation.

6. Mackay, N. (1977) Private communications.

It is obtained by invoking reciprocity and asserting that the variation in coupling for two parallel cables as the frequency is changed will be twice that indicated by Figures 6 and 7. The coupling loss will depend on the cable type and length. For this pulsed system, the illuminated length can be assumed to be equal to about 0.8 $c\tau$, where c is the speed of light and τ is the pulse width.

For this analysis, as will be seen later, only the relative loss designated by $(K_1 - K_o)$ between cable types is of importance. The value for this quantity measured at 60 MHz for the system of Figure 1 is about 30 dB. Its frequency dependence estimated from Figures 6 and 7 is plotted in Figure 8.

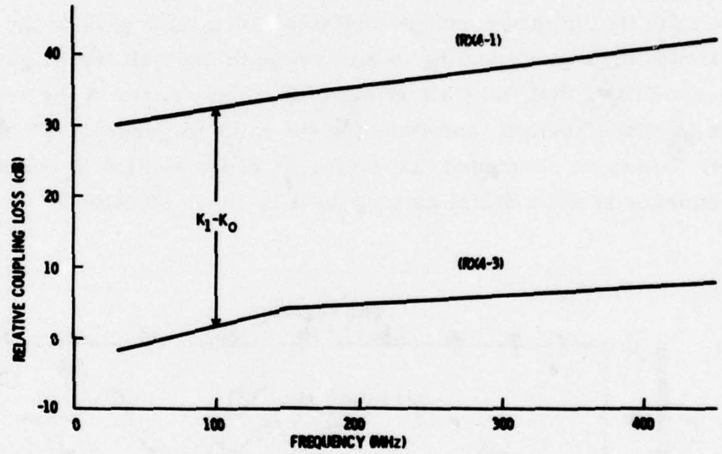

Figure 8. Variation in Relative Coupling Loss with Frequency

4. SCATTERING CROSS SECTION

Very little information is available on the scattering cross section of biological obstacles for frequencies below approximately 300 MHz. These data are of interest only for radar systems which traditionally operate at frequencies from 400 MHz to 10 GHz.

The assignment of a scattering cross section to a target provides a convenient way of quantifying its interaction with an incident electromagnetic field. Implicit in the specification of cross section is the scattering angle θ which allows the computation of the power scattered in that direction. For the radar cross section, θ = 180° and for the forward scattering cross section, θ = 0°. The computation or measurement of scattering cross section is based on the assumption that the target is sufficiently far from the source to ensure that it is uniformly illuminated. However, in the absence of data for the two-cable system, it will be assumed for the purpose of this analysis that response of the system is proportional to the forward-scattering cross section of the intruder.

A number of measurements have been made in order to determine the forward-scattering cross section of an adult for frequencies in the 30- to 450-MHz range. The measurements were made first over a ground plane and then repeated over the earth. The goal was to determine the dependence of the cross section, for various intruder postures, on the frequency of the illuminating signal. The results of some of the measurements for an adult in standing position are shown in Figure 9. Inspection of the curves will show that the cross section when measured over the ground plane exhibits definite resonance effects. The first peak of the response occurs at a frequency corresponding to a wavelength one-half the height of the man. The lower curve shows that the main effect of the lossy earth is the washing out of the structure of cross section, and reducing its value in general. On the basis of these curves, it is to be concluded that so far as cross section is concerned, the operating frequency is not critical as long as it is above 30 MHz.

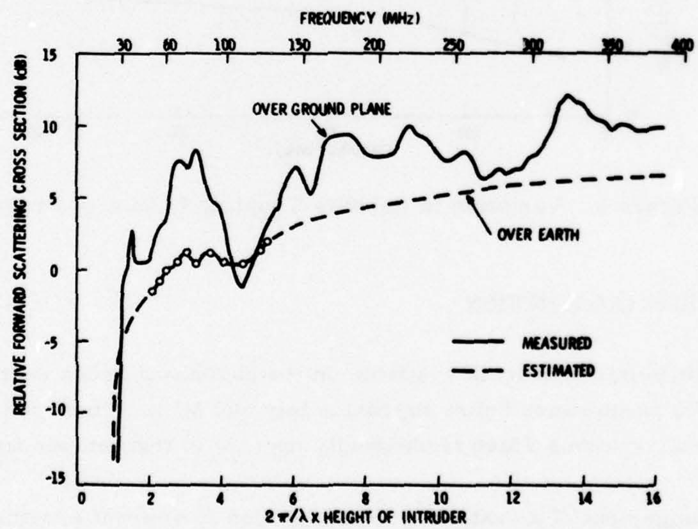

Figure 9. Relative Forward-scattering Cross Section vs Frequency of Standing Adult

The scattering properties of a human frame is a subject also being investigated by workers at Ohio State University,[7] whose initial findings agree in general with the data presented in Figure 9. Using a very short pulse measurement system, they found that a broad peak in the response occurs around 75 to 80 MHz, and that the cross section below 20 to 30 MHz is significantly reduced from its peak value.

5. SENSOR SENSITIVITY

The signal power produced at the receiver input by a target anywhere along the cable can now be estimated by

$$S(\ell, f) = P_o - 2_{AF} - 2A(\ell, f) - K(\ell, f) - C(f) \tag{3}$$

where the dependence on frequency and target location has been indicated. Cable sensitivity is defined as the ratio of the signal power produced by an intrusion at ℓ to that produced by the same intrusion at $\ell = 0$. For cables of uniform hole size $K(\ell, f) = K(f)$ and

$$S(\ell, f) - S(0, f) = -2A(\ell, f) = -2\alpha\ell \tag{4}$$

where α is the attenuation factor shown in Figure 2. The relative sensitivity is plotted in Figure 10 for $\alpha = 0.6$ dB/100 ft and shows that the signal power produced by a disturbance at the far end of the first section is more than 20 dB less than that produced by the same disturbance at the near end.

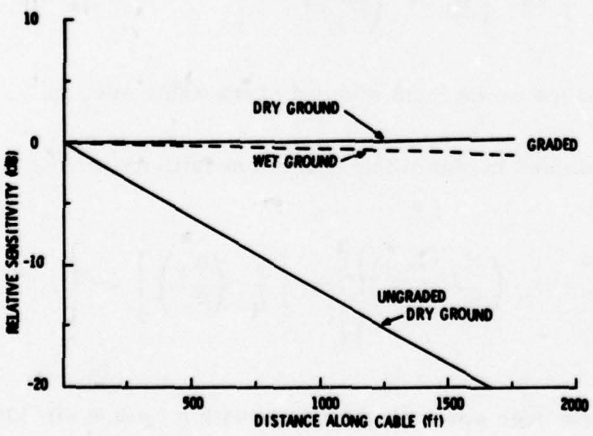

Figure 10. Relative Cable Sensitivity

7. Garbacz, R. (1978) Private communications.

To minimize the variation of relative sensitivity with distance, the cable properties are gradually changed from one end of a section to the other. The coupling loss is decreased with distance to compensate for attenuation, which tends to keep the received signal power more nearly constant. However, as the coupling loss is decreased the attenuation factor increases. If the cable characteristics change from those of RX4-1 at the input end to those of RX4-3 at the end of a section and over the section, the attenuation factor is

$$\alpha(\ell) = \alpha_o \exp\left[\frac{\ell}{L} \ln\left(\frac{\alpha_1}{\alpha_o}\right)\right] \tag{5}$$

where α_o and α_1 are the values corresponding to the beginning and end of the cable, respectively.

Integration of Eq. (5) yields the total attenuation. Thus the two-way attenuation is

$$2A = \frac{2\,\alpha_o L}{\ln\left(\frac{\alpha_1}{\alpha_o}\right)} \left\{ \exp\left[\frac{\ell}{L} \ln\left(\frac{\alpha_1}{\alpha_o}\right)\right] - 1 \right\} \tag{6}$$

which reduces to $2\,\alpha_o L$, the ungraded value for 2A, in the limit of $\alpha_1 \rightarrow \alpha_o$. Offsetting the increasing attenuation is the decrease in coupling loss. With the assumption that the increase in attenuation factor is proportional to the decrease in coupling loss, the coupling loss can be expressed as

$$K(\ell) = K_o + \left(\frac{K_1 - K_o}{\alpha_1 - \alpha_o}\right) \alpha_o \left\{ \exp\left[\frac{\ell}{L} \ln\left(\frac{\alpha_1}{\alpha_o}\right)\right] - 1 \right\} \tag{7}$$

where K_o and K_1 are the coupling losses at the input and end of the cable section, respectively.

Equations (5) and (7) can be combined to obtain the relative sensitivity for the graded cable pair

$$S(\ell, f) - S(o, f) = - \left\{ \frac{2\,\alpha_o L}{\ln\left(\frac{\alpha_1}{\alpha_o}\right)} + \alpha_o \left(\frac{K_1 - K_o}{\alpha_1 - \alpha_o}\right) \right\} \left\{ \exp\left[\frac{\ell}{L} \left(\frac{\alpha_1}{\alpha_o}\right)\right] - 1 \right\}. \tag{8}$$

Equation (8) is plotted in Figure 10 for free space (solid curve) with α_o = 0.6 dB/100 ft, α_1 = 1.2 dB/100 ft, and $K_1 - K_o$ = -31 dB.

The interpretation of Eq. (8) in free space is clear. However, how it should be used when the cables are on or in the ground is not so clear. Equation (6) gives the correct value for the total attenuation independent of cable location as long as the corresponding values for the attenuation factors are used. Equation (7) for the coupling loss is based on the assumption that the coupling loss changes according to the free space attenuation factor. Once the cable is manufactured, is the slope of the grading fixed? There is some evidence, as suggested in Section 3, which indicates that the value of $(K_1 - K_o)$ would tend to increase as the value of $(\alpha_1 - \alpha_o)$ increases due to the cables being near the earth. However, the available evidence (Figure 7) is in no way conclusive and to be consistent with previous remarks, the value of $K_1 - K_o$ will be considered to be independent of cable location. In addition, the shape of the curve expressed by Eq. (7) depends on the values of α_o and α_1 for free space. Thus it must be restricted so that only free space values evaluated at the design frequency (60 MHz) can be used. Thus it is rewritten as

$$K(\ell, f) = K_o + \left(\frac{K_1 - K_o}{\alpha'_{1o} - \alpha'_{oo}}\right) \alpha'_{oo} \left\{ \exp\left[\frac{\ell}{L} \ln\left(\frac{\alpha'_{1o}}{\alpha'_{oo}}\right)\right]\right\} - 1 \tag{9}$$

where the second subscript and the prime mean—evaluated at 60 MHz and free space, respectively.

The relative sensitivity for any condition is then equal to

$$S(\ell, f) - S(o, f) = - \frac{2\,\alpha_o L}{\ln\left(\frac{\alpha_1}{\alpha_o}\right)} \left\{ \exp\left[\frac{\ell}{L} \ln\left(\frac{\alpha_1}{\alpha_o}\right)\right] - 1 \right\} +$$

$$- \left(\frac{K_1 \quad K_o}{\alpha'_{1o} \quad \alpha'_{oo}}\right) \alpha'_{oo} \left\{ \exp\left[\frac{\ell}{L} \ln\left(\frac{\alpha'_{1o}}{\alpha'_{oo}}\right)\right] - 1 \right\} . \tag{10}$$

The relative sensitivity when the cables are on or in the ground, determined from this expression, is plotted as the dashed curve in Figure 10 for $\alpha_o = 0.6$ dB/100 ft and $\alpha_1 = 1.3$ dB/100 ft. A much larger degradation in performance occurs at higher frequencies.

It should be remembered that the curves shown in Figure 10 represent average conditions. The interaction of the waves traveling inside the leaky coaxial cables and the surface waves outside the cables produces regions of greater and lesser sensitivity. Any system design must include a safety factor to allow detection even in the most insensitive regions.

6. NOISE POWER

The total noise power at the receiver mixer is made up of contributions from the matched load that terminates the far end of the receiving cable and the excess noise of the line amplifiers and interconnecting cables. The contribution from radiation is neglected in this analysis. The total noise power can be expressed as

$$N = kBT \frac{G^3}{A_L{}^3 A_F} F_S \tag{11}$$

where K is the Boltzmann constant, B the noise bandwidth, T the temperature in degrees Kelvin (°K), G the gain of the line amplifiers, A_L the loss of a leaky coaxial section, A_F the loss of a feeder cable, and F_S the system noise figure. The system noise figure can be computed with Frii's formula[8]

$$F_s = F_1 + \frac{F_2 - 1}{G_1} + \frac{F_3 - 1}{G_1 G_2} + \ldots \tag{12}$$

For the system represented in Figure 1, $F_2 = F_4 = F_7 = F$ and $G_2 = G_4 = G_7 = G$, the noise figures of the leaky coaxial cables can be represented by

$$F_1 = F_3 = F_5 = 1 + (A_L - 1)\frac{T}{T_o} \tag{13}$$

and that of the feeder cable by

$$F_6 = 1 + (A_F - 1)\frac{T}{T_o} ; \tag{14}$$

T_o is the standard temperature, 290°K. From these expressions F_S is found to be

$$\begin{aligned} F_S = 1 &+ (A_L - 1)\frac{T}{T_o}\left[1 + \frac{A_L}{G} + \frac{A_L{}^2}{G^2}\right] \\ &+ (F - 1) A_L \left[1 + \frac{A_L}{G} + \frac{A_L^2 A_F}{G^2}\right] \\ &+ (A_F - 1)\frac{T}{T_o}\frac{A_L^3}{G^2} . \end{aligned} \tag{15}$$

8. Ziemer, R.E., and Tranter, W.H. (1976) Principles of Communications, Houghton Mifflin Company, Boston, Mass.

The relative noise power at the mixer input was evaluated with Eq. (11) as a function of frequency. The results are plotted in Figure 11 for three temperatures. Variation of the noise power with temperature is not great.

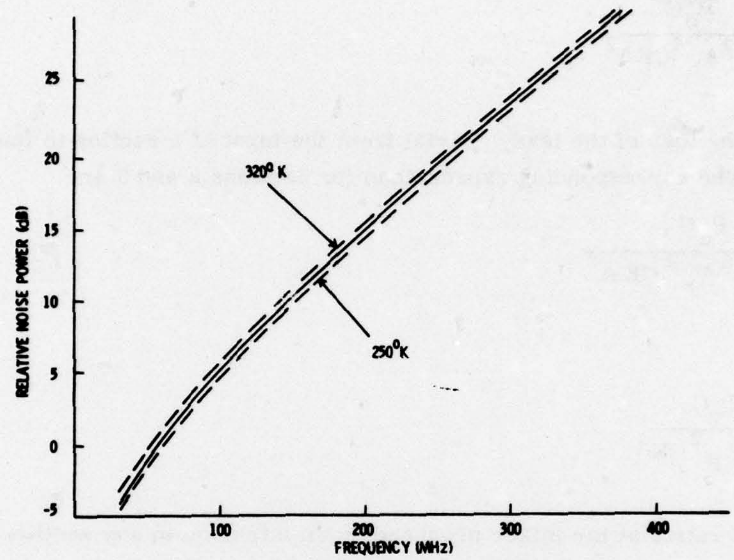

Figure 11. Receiver Noise Power Variation with Frequency and Temperature

The noise figure of a solid state amplifier is independent of frequency over the range of interest here. In practice, its gain is usually set to make up exactly the one-way ported coaxial loss. A noise figure of 3 to 4 dB and a gain of 20 dB are typical for these amplifiers. When the line loss exceeds 20 dB, two amplifiers must be used in each section, further degrading the S/N ratio. The system noise will also tend to vary as the cable attenuation factors change with varying soil conditions. This latter effect is treated in the next section.

7. SIGNAL-TO-NOISE RATIO

It is now possible to use the results of the previous sections to estimate the S/N ratio at any frequency and compare it to that obtained for the Guidar system at 60 MHz.

The signal power which reaches the mixer input depends on the location of intruder target along the cable. As indicated in Figure 1, the section farthest from the receiver is denoted as Section 1. There the signal power produced by an intrusion is

$$S_1 = \frac{P_o G^5}{A_F{}^2 A_L{}^4 CKA^2} \tag{16}$$

where A is the loss of the leaky coaxial from the input of a section to the point of intrusion. The corresponding expressions for Sections 2 and 3 are

$$S_2 = \frac{P_o G^3}{A_L{}^2 A_F{}^2 \, CK A^2} \tag{17}$$

and

$$S_3 = \frac{P_o G}{A^2 A_F{}^2 \, CK} \tag{18}$$

The S/N ratios at the mixer produced by an intrusion in any section are, respectively,

$$\frac{S_1}{N} = \frac{P_o}{kBTCK(F_s/A_L)\,(A_L/G)^2 A_F A^2} , \tag{19}$$

$$\frac{S_2}{N} = \frac{P_o}{kBTCK(F_s/A_L)\, A_F A^2} , \tag{20}$$

$$\frac{S_3}{N} = \frac{P_o}{kBTCK(F_s/A_L)\,(G/A_L)^2 A_F A^2} . \tag{21}$$

It can be seen that when the gain of the amplifiers exactly offsets the ported coaxial loss, $\frac{S_1}{N} = \frac{S_2}{N} = \frac{S_3}{N}$, and the effective S/N ratio is given by Eq. (20).

The ratio of the S/N ratio at any frequency to that at 60 MHz can be expressed as

$$\frac{S/N}{(S/N)_o} = \frac{C_o (K)_o F_{So} \, A_{Fo} A_o{}^2 \, A_L}{CK \, F_S \, A_F A^2 \, A_{Lo}} . \tag{22}$$

Formal substitution of the terms making up this expression can be written in logarithmic notation as

$$
\begin{aligned}
D(\ell, f-f_o) = {} & (A_{Fo} - A_F) + (C_o - C) + (K_{oo} - K_o) \\
& + \frac{2\,\alpha_{oo}\,L}{\ln\left(\dfrac{\alpha_{o1}}{\alpha_{oo}}\right)} \left\{ \exp\left[\frac{\ell}{L}\ln\left(\frac{\alpha_{o1}}{\alpha_{oo}}\right)\right] - 1 \right\} \\
& - \frac{2\,\alpha_o\,L}{\ln\left(\dfrac{\alpha_1}{\alpha_o}\right)} \left\{ \exp\left[\frac{\ell}{L}\ln\left(\frac{\alpha_1}{\alpha_o}\right)\right] - 1 \right\} \\
& + \left\{ K_{1o} - K_{oo}) - (K_1 - K_{oo}) \right\} \left\{ \frac{\alpha'_{oo}}{\alpha'_{1o} - \alpha'_{oo}} \right\} \left\{ \exp\left[\frac{\ell}{L}\ln\left(\frac{\alpha'_{1o}}{\alpha'_{oo}}\right)\right] - 1 \right\} \\
& + (F_{So} - F_S) + (A_L - A_{Lo}) \,.
\end{aligned}
\tag{23}
$$

In this expression, the explicit frequency dependence of each factor is not indicated except that the second subscript should be taken to mean—at 60 MHz. The first subscript, o or 1, means the beginning or end of the cable, respectively. Measured or estimated values for each of the quantities in Eq. (23) have been given in previous sections; these values are summarized for a number of frequencies in Table 1.

Equation (23) was evaluated both for dry ground and wet ground conditions, with the results presented in Figures 12 and 13. It can be seen from these figures that the S/N ratio drops sharply as the frequency is increased. This degradation in performance is produced by the decrease in signal power coupled with the simultaneous increase in noise power.

The present Guidar system used as a benchmark in this analysis has a signal margin no greater than 10 dB. This means that a relative S/N ratio of -10 dB or less makes operation of the system at that frequency impossible. For example, Figure 12 shows that at 80 MHz, system performance becomes inadequate at ranges greater than about 900 feet. Performance is further degraded if the ground is wet. Figure 12 shows that at 80 MHz, maximum range is limited to about 1200 ft and operation at 100 MHz is not possible.

Table 1. Values of Parameters Used to Evaluate System Performance

Freq. (MHz)	Attenuation Factor (dB/100 ft)						Relative Coupling Loss (dB)		Relative Cross Section (dB)
	Dry Ground		Wet Ground		Low Loss				
	α_o	α_1	α_o	α_1	α_o	α_1	$K_1 - K_o$	$K_{oo} - K_o$	$C_o - C$
30	0.4	0.9	0.4	1.0	0.25	0.70	-32	1	-6
60	0.6	1.2	0.6	1.3	0.33	0.90	-31	0	0
80	0.7	1.3	0.7	1.7	0.49	1.05	-30	-1	0
100	0.8	1.5	0.8	2.1	0.45	1.25	-30	-1	0
150	1.1	1.9	1.1	3.1	0.60	1.50	-30	-3	3
200	1.2	2.2	1.3	4.0	0.70	1.75	-31	-4	5
250	1.4	2.6	1.5	5.0	0.75	2.05	-32	-6	5
300	1.6	3.0	1.7	6.0	0.85	2.30	-32	-7	6
350	1.7	3.3	1.9	7.0	0.92	2.55	-33	-8	6
400	1.9	3.6	2.1	8.0	1.00	2.85	-33	-10	6
450	2.1	4.0	2.3	9.0	1.10	3.10	-34	-11	6

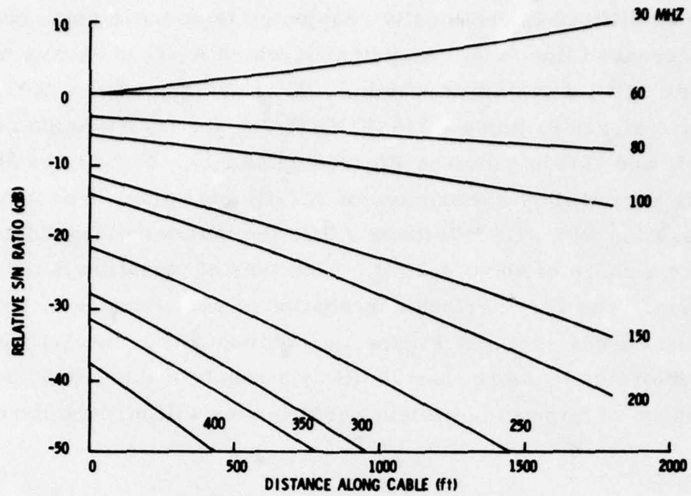

Figure 12. Relative S/N Ratio for Dry Ground

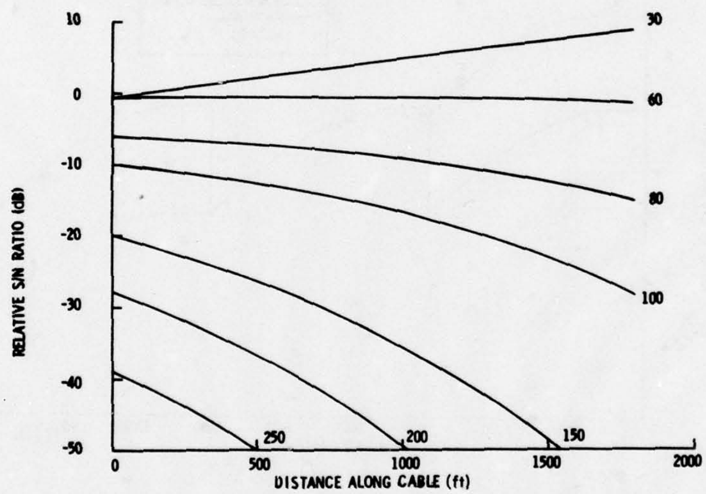

Figure 13. Relative S/N Ratio for Wet Ground

Figures 12 and 13 give the performance in Section 3 of the system. The performance of subsequent sections relative to this one can be found from Eqs. (19), (20), and (21). But first some additional factors must be considered. In practice, the system might be set up for dry ground conditions with gains of the line amplifiers set to equal the attenuation in a section of line. If the ground conditions change, the cable attenuation will increase, producing a change in the S/N ratio. The magnitude of this change in each section depends on the operating frequency and whether or not the gain of the amplifiers is continually readjusted (automatic gain control [AGC]) to match the increased line loss. A system in which A_1/G is always unity is designated—with AGC; a system in which A_L/G is designated—no AGC.

The relative signal-to-noise ratio $(S/N)/(S/N)_o$ for each section computed from Eqs. (19), (20), and (21) is shown in Figures 14 and 15. For 30 and 60 MHz, system performance is degraded by a maximum of 2.2 dB and varies over a range of about 1.5 dB for operation with AGC. Without AGC, the maximum degradation is 3.6 dB and varies over a range of about 4.2 dB. This type of variation is not serious in a practical system. The very serious degradation of performance at 100 MHz is evident from the curves shown in Figure 15. Without AGC, the S/N ratio in Section 1 has deteriorated by more than 20 dB as a result of the ground being wet.

Some methods of improving system performance will be considered in the next section.

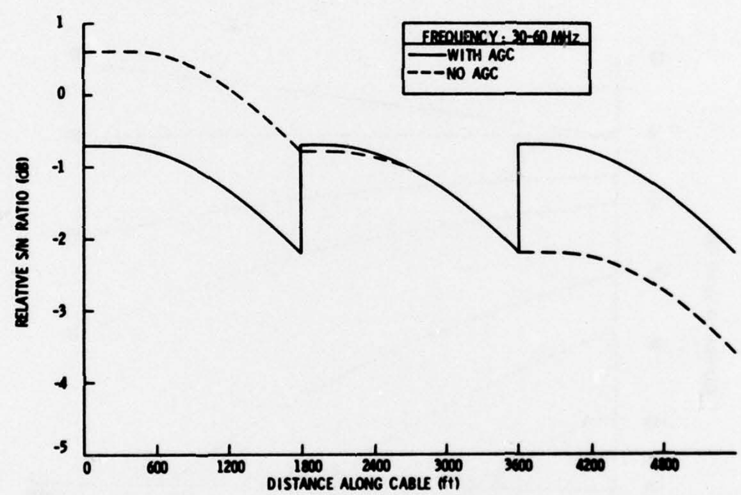

Figure 14. Intersection Variation of S/N Ratio with Wet Ground for 60 MHz

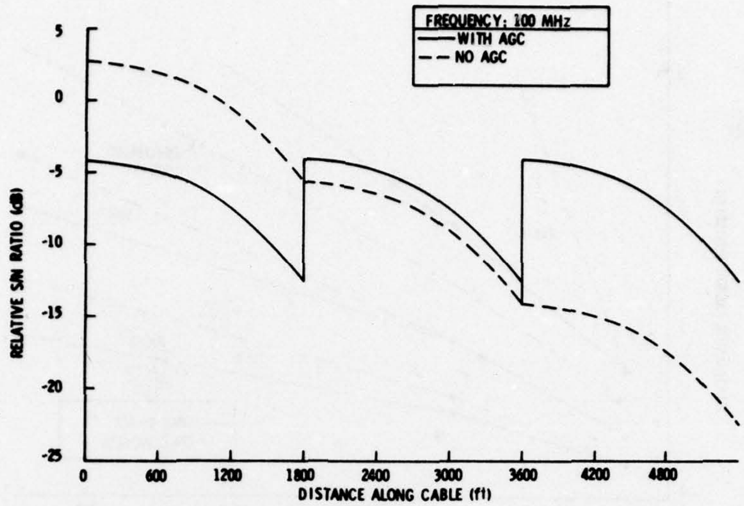

Figure 15. Intersection Variation of S/N Ratio with Wet Ground for 100 MHz

8. DISCUSSION

The results of the preceding calculations show that for best performance, the operating frequency of guided wave radar systems like Guidar should be below about 75 MHz. To obtain equivalent performance at higher frequencies some system modification would be required. One such change would be to raise the transmitter power. Although a further increase in transmitter power is possible, electromagnetic compatibility problems might arise. These guided wave radar systems are broad band pulsed systems. They typically operate at bandwidths of around 2 MHz and are sources of potential interference in the VHF television band. The transmitting Radiax cable is an extremely inefficient antenna so very little power is actually radiated and no TVI problems would be anticipated with peak power levels of one or two watts. Significantly higher levels, however, could lead to interference problems in some areas.

Since the degradation in performance is due to the attenuation of the cables, use of lower loss cables would be the most direct way to improve performance. The attenuation factor for RX5-1, a larger diameter but lower loss Radiax cable, is shown in Figure 16. Comparison with the curves for RX4-1 clearly shows its lower attenuation. The RX5-1 cable has a 7/8-in. diam compared to 1/2-in. for RX4-1 cable. However, its coupling loss is about the same as that of RX4-1. The curve marked "estimated" in Figure 16 is assumed for the low-loss version of RX4-3.

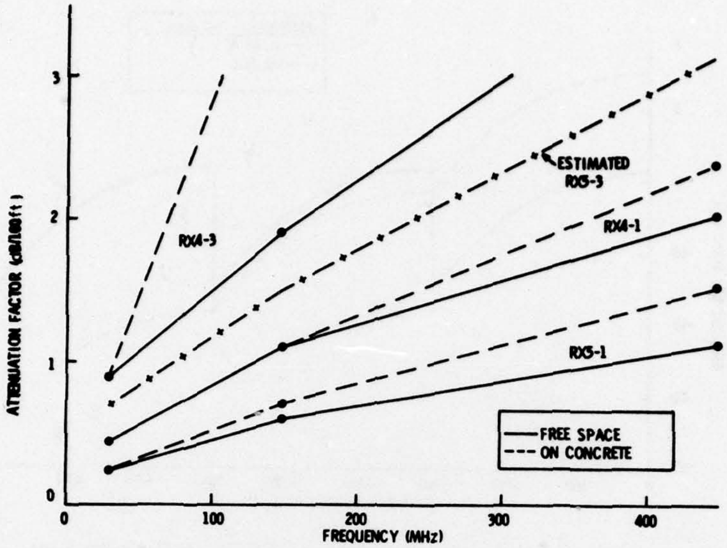

Figure 16. Comparison of Attenuation Factors for Standard and Low-loss Cables

The relative S/N ratio for a system using this type of cable was evaluated with Eq. (23) assuming no other system parameter changes except the smaller cable attenuation. The results shown in Figure 17 demonstrate the marked improvement in system performance. Performance at 100 MHz with low-loss cable is in fact better than that achieved with the old cable at 60 MHz. Additional transmitter power could also be used with this cable to improve performance still more. The total attenuation for an 1800-ft section of sensor cable is shown in Figure 18 for both RX-4 and RX-5 cable types. The lower attenuation for RX-5 is apparent.

The Andrew Company has developed a low-loss dielectric for its Radiax cables, providing a significant reduction in attenuation factor. Attenuation factors previously achieved with 7/8-in. diam cables can now be obtained with the 1/2-in. cables. Thus a significant range of operating frequencies now appears possible without incurring the high cost penalty associated with the larger cable.

Another more important aspect of low-loss cables is the increase in the length of a section which may be possible before a line amplifier is required. The line amplifiers represent a potential source of false alarms, require maintenance, and increase system life-cycle cost. Their elimination would represent a very significant improvement in system performance and reliability. However, these new low-loss cables have not yet been evaluated in this application.

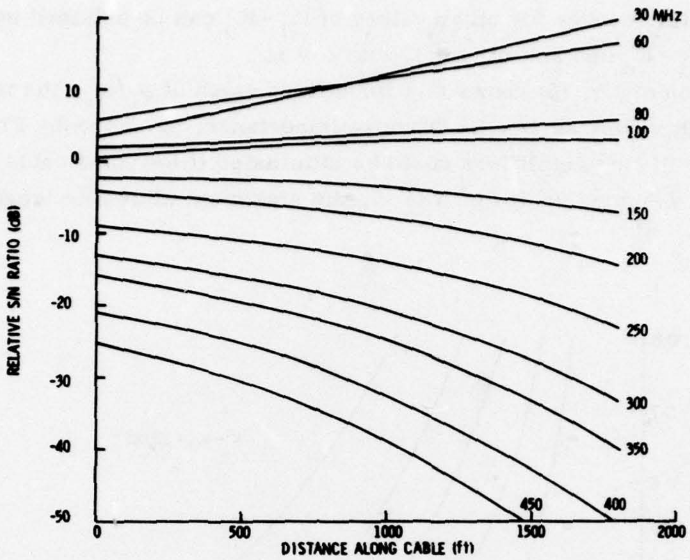

Figure 17. Relative S/N Ratio for Low-loss Cables in Dry Ground

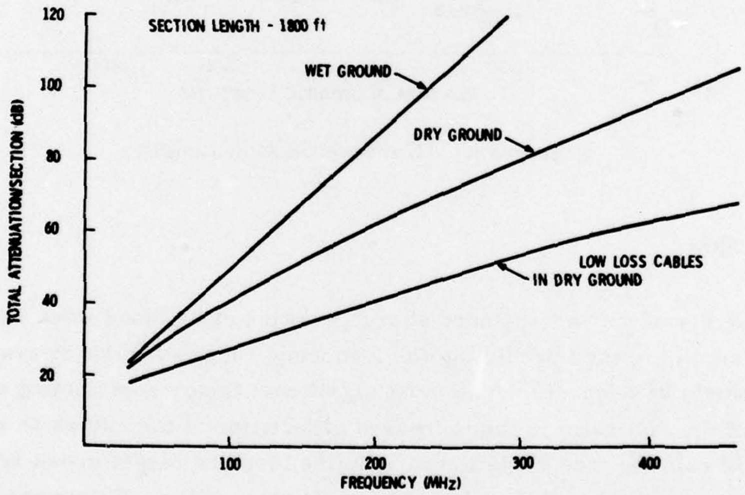

Figure 18. Comparison of Attenuation for Standard and Low-loss Cables

The curves shown in Figure 19 give an indication of the length per section that is possible as a function of the cable parameters. These curves apply only to the case where the difference in coupling between the start and end grading of the cable is 32 dB. Similar curves for other values of $K_1 - K_o$ can be obtained by setting 2A in Eq. (6) to $K_1 - K_o$ and solving for L with ℓ = L.

Examination of Eq. (6) shows that for a fixed value of α_1/α_o, the maximum allowable length varies as $1/\alpha_o$. Of more importance, as shown by Figure 19, is the fact that all line amplifiers could be eliminated if low-loss cable were used. For the assumed values of RXY-5, the maximum allowable length is about 8000 feet.

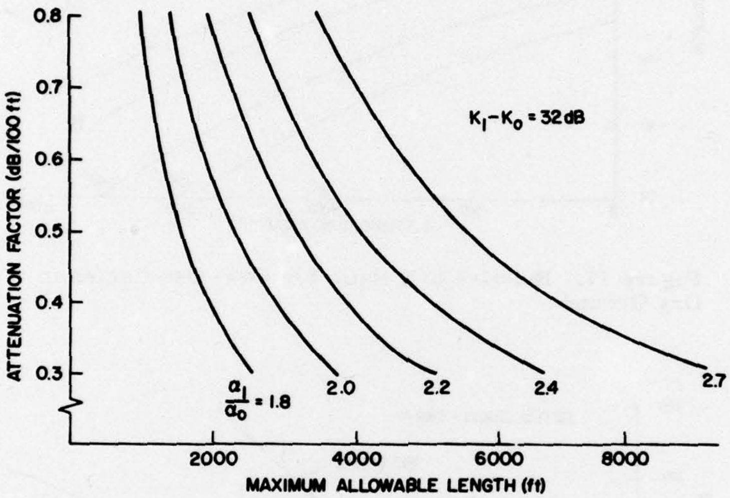

Figure 19. Allowable Section Length

9. CONCLUSION

An analysis of the performance characteristics of a guided wave radar has been given with an aim toward predicting the frequency range over which system performance would be adequate. The most significant factor contributing to the degradation of the S/N ratio is the increased attenuation of the cables as the operating frequency is raised. The variation in coupling loss and target cross section is unimportant compared to the variation in cable attenuation. To overcome the attenuation, the transmitter power could be increased. A lower loss ported coaxial cable would greatly improve system performance at 60 MHz, allow the elimination of some or all of the line amplifiers, or allow operation at higher frequencies. It is apparent from Figure 15 that AGC must be incorporated in systems designed to operate at higher frequencies with lossy cables in order to limit the degradation of the signal-to-noise ratio for the far out cable sections. It should also be remembered that the S/N ratios that were obtained represent averages. The particular value measured at any point could be higher or lower than the average, depending on the intercable coupling loss and ground conditions there. With the equations given, system performance can be estimated for various configurations; for example, to evaluate the impact of using a sensor made up of one high-loss and one low-loss cable. The variation of S/N ratio can be computed for various amplifier gain control methods, or for the effect of various grading and coupling loss profiles.

The curves shown in Figure 19 provide a convenient method of estimating the section length from the cable parameters. These curves show that sections of one mile or longer would be possible without line amplifiers.

References

1. Harman, R.K. (1976) GUIDAR: An intrusion detection system for perimeter protection, Proc. 1976 Carnahan Conference on Crime Countermeasures University of Kentucky, Lexington, Ky.
2. Bulletin 1058A, Radiax Slotted Coaxial Cable, Andrew Corporation, Orland Park, Ill.
3. Catalog 28, Antennas/Transmission Lines, Andrew Corporation, Orland Park, Ill.
4. Cree, D.J., and Giles, L.J. (1975) Practical performance of radiating cables, Radio Elec. Eng. **45**(No. 5):221-225.
5. Yoh, P., Esposito, R., Gagnon, R., and Kodis, R.D. (1974) Measurements of Leaky Coaxial Cables and Possible Applications to Train Communications, Report No. FRA-ORD&D-74-43, U.S. Department of Transportation.
6. Mackay, N. (1977) Private communications.
7. Garbacz, R. (1978) Private communications.
8. Ziemer, R.E., and Tranter, W.H. (1976) Principles of Communications, Houghton Mifflin Company, Boston, Mass.